J|A|C|S COMMUNICATIONS

Published on Web 12/09/2009

Reactivity of TiO_2 Rutile and Anatase Surfaces toward Nitroaromatics

Shao-Chun Li* and Ulrike Diebold*

Department of Physics and Engineering Physics, Tulane University, New Orleans, Louisiana 70118

Received September 16, 2009; E-mail: sli1@tulane.edu; diebold@tulane.edu

Ever since the discovery of low-temperature oxidation of carbon monoxide by TiO_2-supported Au nanoparticles (Au/TiO_2),[1] this catalytic system has fascinated researchers in applied and fundamental areas. The roles of the nanoparticles, the support, and the interaction between the two are still very much debated.[2] Recently, it was reported that Au/TiO_2 also acts as a high-yield catalyst for the synthesis of aromatic compounds,[3,4] specifically the chemoselective reduction of nitroaromatics to aniline[3] and the synthesis of azobenzene via oxidation of anilines. It was also postulated that a more defective TiO_2 support, containing O vacancies or other defects, enhances the catalytic performance.[4] Interestingly, non-Au promoted TiO_2 was also shown to be effective and highly selective in azobenzene synthesis, albeit with a lower conversion efficiency.[4]

In this work, we provide evidence that TiO_2 by itself cleaves the N═N double bond of azobenzene, leading to a phenyl imide (C_6H_5N) intermediate organized in an ordered superstructure. Adsorption of aniline results in the same superstructure, composed of the same (or very similar) intermediate. As a consequence it is suggested that, in the Au-sensitized catalyst, the main role of the Au could be to activate the O_2/H_2 reactants and, via a (de)hydrogenation of the TiO_2 support, facilitate the coupling of phenyl imide to azobenzene or its desorption as aniline, respectively.

The experiments were performed in two separate ultrahigh vacuum chambers (UHV, base pressure $\sim 1 \times 10^{-10}$ mbar), one equipped with an Omicron room temperature (RT) scanning tunneling microscope (STM) and Low Energy Electron Diffraction (LEED), and the other one with X-ray Photoemission Spectroscopy (XPS, SPECS Phoibos 150) and an Omicron STM/AFM. Two TiO_2 crystals, anatase (101) and rutile (110), were cleaned by a standard procedure consisting of cycles of Ar^+ ion sputtering plus annealing to ~600 °C. Surface cleanliness was checked prior to the experiments (see Figure S1). The azobenzene (orange color) and aniline (yellowish color) were purified using freeze−pump−thaw cycles prior to dosing into the UHV and characterized with mass spectrometry. The TiO_2 samples were kept at RT, and the pressure remained below 1.5×10^{-8} mbar during dosing. All measurements were carried out at RT. Empty-states STM scans were performed in constant current mode. For the XPS measurements a Mg Kα anode was used. Surface oxygen vacancies (O_V^{surf}) do not need to be considered for either sample: while the rutile (110) surface contains O_V^{surf} (~5%) right after sample preparation, these were filled by hydroxyl groups via water dissociation from the residual gas in our case; the anatase (101) surface has been found to contain subsurface intrinsic defects rather than O_V^{surf}.[5] Our sample preparation procedures do result in a reduced bulk for both TiO_2 samples, however.

Figure 1a shows an STM image taken after dosing ~0.02 monolayers (ML, 1 ML ≈ 2.58×10^{14} /cm^2, here defined as half of the surface unit cells) azobenzene on the anatase (101) surface. Each molecule appears as a dumbbell-shaped feature, located at the surface 5 coordinated Ti (Ti_{5c}) rows with its axis oriented along,

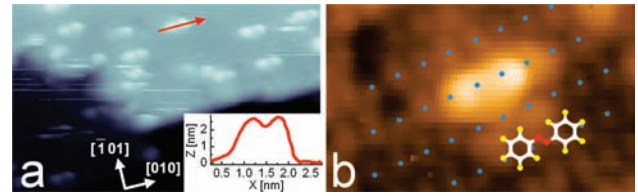

Figure 1. STM images of a low coverage of azobenzene on TiO_2 anatase (101). (a) $U_{sample} = +1.85$ V, $I_{tunnel} = 0.2$ nA, 15 nm × 10 nm. Each dumbbell feature is assigned to a single azobenzene molecule; the streakiness indicates mobile species. The line profile in the inset was taken at the position of the red arrow. (b) $U_{sample} = +1.55$ V, $I_{tunnel} = 0.25$ nA, 4.5 nm × 2.5 nm. An individual azobenzene molecule together with a schematics of the proposed adsorption configuration. Blue dots indicate the position of surface Ti_{5c} sites.

but slightly deviating from, the [010] direction. This is seen more clearly in the high-resolution image in Figure 1b. At RT, the dumbbell-shaped feature diffuses rather fast as an entity; the 'noisy' lines in Figure 1a are due to the rapid motion of the adsorbates between the surface and STM tip. This is a strong indication that the azobenzene molecule has not dissociated. The two protrusions of the dumbbell have almost equivalent apparent heights, and the maxima are separated by ~6.6 Å, consistent with the energetically favorable planar *trans*-isomer typically observed on close-packed metal surfaces.[6−8] The azobenzene moves even faster on the rutile (110) surface, where single molecules could not be resolved at RT.

At saturation coverage the azobenzene exhibits a quite different morphology. STM images reveal ordered periodic protrusions with nearly identical height and shape (Figure 2). New superstructures are observed on both anatase (101) and rutile (110) at full coverage. The dumbbell-shaped features, corresponding to azobenzene molecules at low coverage, are no longer present in Figure 2a−d. This is distinctly different from the azobenzene islands observed on transition metal surfaces,[7] where the dumbbell shape is preserved for high local coverages. LEED confirms that azobenzene forms superstructures with a p(2 × 1) and c(2 × 2) symmetry on anatase (101) and rutile (110), respectively (Figure 2e and f). The azobenzene overlayer on anatase consists of two domains, as indicated by the two sets of reciprocal vectors in LEED (red and blue arrows in Figure 2e). On rutile (110) only one type of domain boundary was (occasionally) observed, running straight along the [001] direction with one lattice unit offset between neighboring domains (not shown). According to the STM and LEED results, each protrusion occupies two substrate lattice sites along the [010] and [001] directions for anatase (101) and rutile (110), respectively.

Is each bright protrusion in the superstructures due to an azobenzene molecule, or does the molecule split into two phenyl imide (C_6H_5N) groups? The following results indicate that the latter is the case.

Aniline ($C_6H_5NH_2$) is structurally similar to phenyl imide, except for two extra hydrogen atoms at the N group. Adsorption of aniline at RT (Figure S2) shows that aniline forms the same superstructures

 10.1021/ja907865t

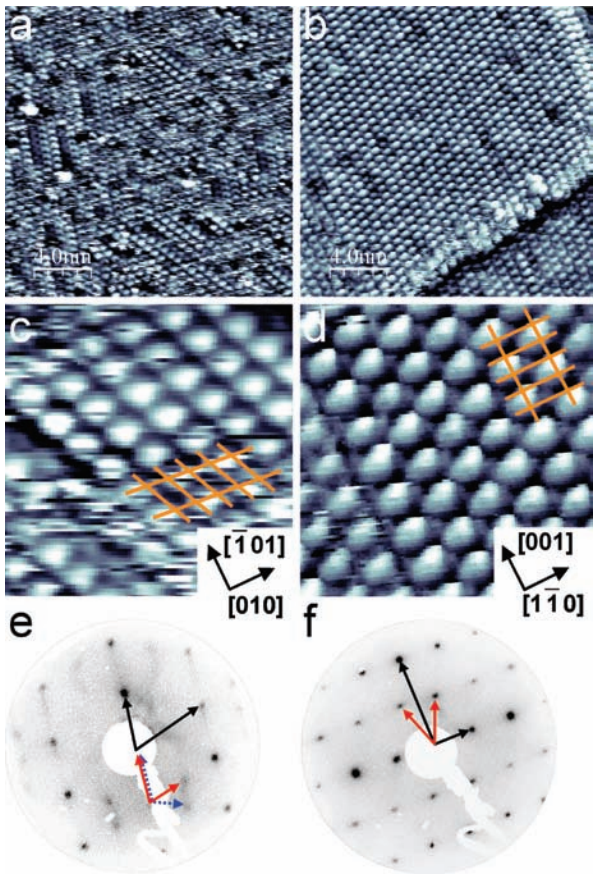

Figure 2. Saturation coverage of azobenzene on TiO_2 anatase (101) (left panels) and rutile (110) (right panels). (a, b) STM images (20 nm × 20 nm), (a) $U_{sample} = +1.3$ V, $I_{tunnel} = 0.2$ nA and (b) $U_{sample} = +1.2$ V, $I_{tunnel} = 0.2$ nA). (c, d) Zoomed-in STM images (5 nm × 5 nm). The substrate 1 × 1 lattices are superimposed by orange lines. (e, f) LEED patterns ($E = 55$ eV). Black arrows represent the primitive reciprocal lattice vectors of the substrate and colored arrows show the (e) p(2 × 1) superstructure for anatase (101) composed of two domains and (f) c(2 × 2) superstructure for rutile (110).

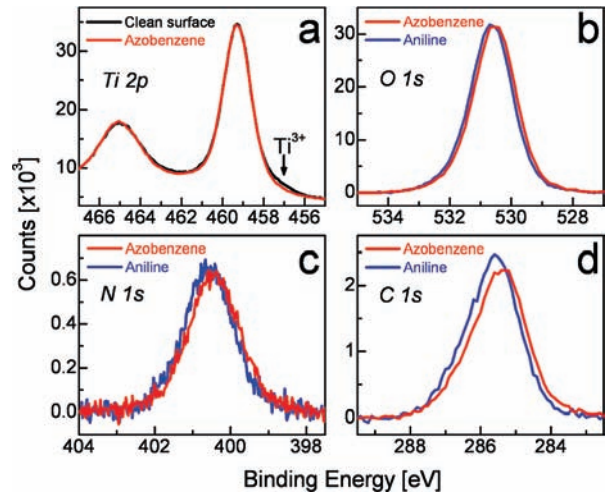

Figure 3. XPS of a saturation coverage of azobenzene and aniline on rutile (110). (a) The Ti*2p* peaks for the clean surface (black line) and after dosing with azobenzene (red line), aligned and normalized to point out the suppression of Ti^{3+} states upon adsorption. The (b) O*1s*, (c) N*1s*, and (d) C*1s* of a saturation coverage of azobenzene (red line) and aniline (blue line).

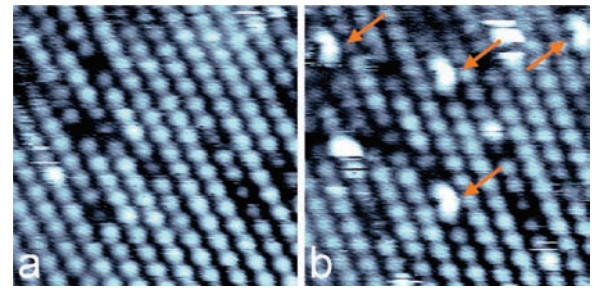

Figure 4. STM images (8.5 nm × 8.5 nm, $U_{sample} = +1.2$ V, $I_{tunnel} = 0.2$ nA) (a) before and (b) after repeated STM scans on the same area of a full layer of azobenzene/rutile (110). Arrows in (b) mark the positions where two phenyl imide groups recombine.

as azobenzene on both anatase (101) and rutile (110). LEED (Figure S2e and f) confirms the respective p(1 × 2) and c(2 × 2) periodicities for the two samples.

XPS measurements (Figure 3) show that, at saturation, the N*1s* and C*1s* peaks of aniline and azobenzene have virtually the same intensity; note that the peaks in Figure 3b−d have not been normalized. The C/Ti ratio was determined as ca. 12%. By comparing this intensity ratio with a full layer of catechol on rutile (110) previously characterized by us,[9] we assert that each bright, periodically arranged protrusion in Figures 2, S2 indeed represents an entity with one phenyl group rather than an azobenzene molecule with two phenyls.

This is also supported by STM-induced recombination reactions, which were occasionally observed (Figure 4). After repeatedly scanning the same area, a few neighboring protrusions are converted into a dumbbell-shaped feature (Figure 4b), which is similar to the molecularly adsorbed azobenzene at low coverage. The STM-induced recombination might be induced by the excitation due to tunneling electrons or the electric field provided by the STM tip.[7,8] We cannot ascertain if these double features reflect an azobenzene molecule or if another species has formed, but this observation certainly confirms that each bright feature in the original structure is due to one phenyl-containing species.

In TiO_2 the Ti has a (formal) oxidation state of 4+ and, in a completely ionic picture, no electrons are available to bind the N of the phenyl imide intermediate to Ti_{5c} sites. The Ti*3d* levels are hybridized with the O*2p* states, however, and the Ti−O bonding has a high degree of covalency. In addition, our TiO_2 samples are slightly bulk-reduced, resulting in intrinsic n-type doping. Some of these excess electrons are localized at subsurface defects and at hydroxyls, resulting in a small Ti^{3+} shoulder in XPS (see black curve in Figure 3a). When azobenzene is adsorbed to the surface, this Ti^{3+} shoulder is suppressed (red curve Figure 3a). Similar substrate → overlayer charge transfer also occurs for other adsorbates on TiO_2, such as Cl and S.[10]

While dissociation of azobenzene can only result in two phenyl imide groups, from STM one cannot tell how many H's are split off from the $-NH_2$ end group of the adsorbed aniline molecule. XPS shows that the N*1s* and C*1s* peak positions are rather similar for the saturated aniline and azobenzene layers, however, except for a small shift of *all* XPS peaks by 0.1 eV to higher binding energies for aniline (Figure 3). Such a rigid shift of the whole XPS spectrum points toward a more downward band-bending in the presence of aniline, rather than a chemical shift indicative of two different chemical species. When aniline splits off hydrogen upon adsorption, the H likely transfers to 2-fold coordinated O_{2c} atoms that act as Brønsted bases. The resulting hydroxyls would then bend the bands downward. The disappearance of the Ti^{3+} shoulder upon adsorption of azobenzene (Figure 3a) is not apparent for aniline (Figure S3), probably because the H reduces the surface, counter-

Scheme 1. Reaction Model of Azobenzene and Aniline on TiO_2

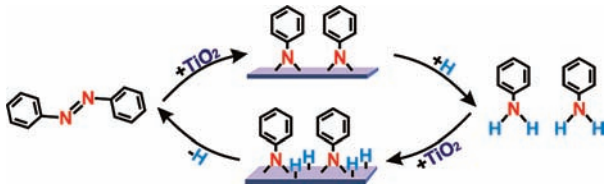

acting the oxidation by the phenyl imide. While these subtle changes do indicate the presence of hydroxyls, we cannot quantify how many of them are present at the surface. Recent experiments on both rutile and anatase show that atomic H can also move to subsurface quite readily,[11] so the bulk has to be considered as a reservoir for H as well.

Since we observe intact azobenzene molecules for small coverages (Figure 1), and the molecule is clearly dissociated in the full layer, it is interesting to speculate how the N═N bond cleavage occurs. A possible adsorption process could be as follows: At low coverage, an isolated azobenzene is molecularly adsorbed on the substrate Ti_{5c} rows, in the energetically favorable *trans*-isomer conformation. (ii) As the coverage increases, the enhanced intermolecular lateral interaction flips up the phenyl rings of the azobenzene to release repulsive energy, presumably similar to the promoted *trans*−*cis*-isomerization in gas phase/on surfaces. (iii) Because of this geometrical change, the hybridization between N═N and Ti_{5c} sites is likely strengthened, which is compensated by the weakened π-states coupling of the phenyl rings to the substrate. This facilitates the N═N cleavage. Electron transfer[8] to the azobenzene may also promote the *trans*−*cis* isomerization. At saturation coverage, the TiO_2 cleaves all the N═N double bonds, producing the phenyl imide, with the terminal N atom bonded to undercoordinated substrate Ti sites.

We have followed the XPS signals while azobenzene was dosed in small increments on the rutile(110) surface (Figure S4). Small, but distinct, changes in the XPS peaks are observed. In particular the N*1s* peak shifts to lower binding energies at a coverage of ~0.5 ML, which could support a coverage-dependent dissociation. For small coverages the C*1s* peak (Figure 4b) is broad and more asymmetric than for higher coverages, possibly because of the more intimate contact betwen the phenyl ring and the substrate in the initial, more flat configuration of the molecule.

The azobenzene cleavage/aniline dissociation takes place on both TiO_2 polymorphs; the different symmetries of the ordered overlayers reflect just the different symmetries of the surface unit cell of anatase (101) and rutile (110). The reactions do not appear to be structure sensitive, as the $Ti_{5c}-Ti_{5c}$ distances and the $Ti_{5c}-O_{2c}$ separations are quite different for the surfaces of these two polymorphs. Particular surface or subsurface defect sites, such as O_V^{surf} or OH groups on rutile (110), and subsurface O_V or Ti interstitials on anatase (101), are not found to play a dominant role in the cleavage/dissociation process for either anatase or rutile, although XPS does indicate that the excess charge in our reduced samples is donated to the phenyl imide intermediate.

Based on the observed TiO_2-induced azobenzene cleavage and aniline dissociation, the mechanism for Au/TiO_2 catalyzed aromatic compound synthesis (aniline → azobenzene/azobenzene → aniline) can be reassessed, as illustrated in Scheme 1. In both cases a similar intermediate is formed and bonded to the substrate Ti_{5c} sites. The only difference is the presence of H for the aniline case, presumably bound to surface oxygen atoms. An essential step for formation of either aniline or azobenzene from this intermediate is then to remove/introduce hydrogen from/onto the surface. For aerobic aniline oxidation, Au/TiO_2 activates O_2 to react off the surface hydroxyls that are produced by aniline dissociation; this leaves only phenyl imide (C_6H_5N), which can combine to form azobenzene. Conversely, for the hydrogenation of azobenzene, Au/TiO_2 activates H_2, which spills over to form hydroxyls at the surface bridging oxygen atoms. These then react with the phenyl imide produced by azobenzene cleavage, resulting in aniline. The observation that PtAu clusters on TiO_2 promote hydrogenation reactions[12] confirms this scenario.

In summary, TiO_2 anatase (101) and rutile (110) surfaces have been demonstrated to cleave the N═N double bond of azobenzene, forming ordered superstructures of phenyl imide (C_6H_5N) on TiO_2—p(1 × 2) on anatase and c(2 × 2) on rutile. Aniline adsorption leads to the same superstructures and the same (or very similar) reaction intermediate. Our observation, namely that TiO_2 is not only a support but also directly capable to catalyze essential steps in (de)hydrogenation reactions of aromatic compounds should help in guiding the further exploration of practical high-yield TiO_2-based and supported catalysts.

Acknowledgment. This work was supported by the Department of Energy (DE-FG02-05ER15702).

Supporting Information Available: Clean TiO_2 anatase (101) and rutile (110) surfaces; superstructures of saturated adsorption of aniline on both anatase (101) and rutile (110) surfaces; XPS data for clean rutile (110) and saturated adsorption of aniline on rutile (110); coverage-dependent XPS data of N*1s* and C*1s* for azobenzene on rutile (110). This material is available free of charge via the Internet at http://pubs.acs.org.

References

(1) Haruta, M. *Catal. Today* **1997**, *36*, 153.
(2) Valden, M.; Lai, X.; Goodman, D. W. *Science* **1998**, *281*, 1647. Freund, H.-J. *Surf. Sci.* **2002**, *500*, 271. Vijay, A.; Mills, G.; Metiu, H. *J. Chem. Phys.* **2003**, *118*, 6536. Molina, L. M.; Rasmussen, M. D.; Hammer, B. *J. Chem. Phys.* **2004**, *120*, 7673.
(3) Corma, A.; Serna, P. *Science* **2006**, *313*, 332.
(4) Grirrane, A.; Corma, A.; Garcia, H. *Science* **2008**, *322*, 1661.
(5) He, Y.; Dulub, O.; Cheng, H.; Selloni, A.; Diebold, U. *Phys. Rev. Lett.* **2009**, *102*, 106105.
(6) Miwa, J. A.; Weigelt, S.; Gersen, H.; Besenbacher, F.; Rosei, F.; Linderoth, T. R. *J. Am. Chem. Soc.* **2006**, *128*, 3164.
(7) Comstock, M. J.; Levy, N.; Kirakosian, A.; Cho, J.; Lauterwasser, F.; Harvey, J. H.; Strubbe, D. A.; Fréchet, J. M. J.; Trauner, D.; Louie, S. G.; Crommie, M. F. *Phys. Rev. Lett.* **2007**, *99*, 038301. Alemani, M.; Peters, M. V.; Hecht, S.; Rieder, K.-H.; Moresco, F.; Grill, L. *J. Am. Chem. Soc.* **2006**, *128*, 14446.
(8) Henzl, J.; Mehlhorn, M.; Gawronski, H.; Rieder, K.-H.; Morgenstern, K. *Angew. Chem., Int. Ed.* **2006**, *45*, 603. Henningsen, N.; Rurali, R.; Franke, K.; Fernández-Torrente, I.; Pascual, J. *Appl. Phys. A* **2008**, *93*, 241. Choi, B.-Y.; Kahng, S.-J.; Kim, S.; Kim, H.; Kim, H. W.; Song, Y. J.; Ihm, J.; Kuk, Y. *Phys. Rev. Lett.* **2006**, *96*, 156106.
(9) Jacobson, P.; Li, S.-C.; Wang, C.; Diebold, U. *J. Vac. Sci. Technol. B* **2008**, *26*, 2236. Li, S.-C.; Wang, J.-g.; Jacobson, P.; Gong, X. Q.; Selloni, A.; Diebold, U. *J. Am. Chem. Soc.* **2009**, *131*, 980.
(10) Hebenstreit, E. L. D.; Hebenstreit, W.; Diebold, U. *Surf. Sci.* **2000**, *461*, 87. Vogtenhuber, D.; Podloucky, R.; Hebenstreit, E. L. D.; Hebenstreit, W.; Diebold, U. *Phys. Rev. B* **2002**, *65*, 1.
(11) Yin, X.-L.; Calatayud, M.; Qiu, H.; Wang, Y.; Birkner, A.; Minot, C.; Wöll, C. *ChemPhysChem* **2008**, *9*, 253. Panayotov, D. A.; Yates, J. T. *Chem. Phys. Lett.* **2007**, *436*, 204.
(12) Serna, P.; Concepción, P.; Corma, A. *J. Catal.* **2009**, *265*, 19.

JA907865T